Science of the Total Environment 541 (2016) 468–482

Contents lists available at ScienceDirect

Science of the Total Environment

journal homepage: www.elsevier.com/locate/scitotenv

Hydrochemistry of inland rivers in the north Tibetan Plateau: Constraints and weathering rate estimation

Weihua Wu

Key Laboratory of Surficial Geochemistry, Ministry of Education, School of Earth Sciences and Engineering, Nanjing University, Nanjing 210093, China

HIGHLIGHTS

- TDS in the inland rivers are 10 times higher than the mean value of world rivers.
- Contribution of evaporite to TDS is >50% in most of the inland rivers.
- Silicate weathering rates in inland rivers are evidently lower than exorheic rivers.
- Weathering rates in various regions of the Tibetan Plateau are noticeably different.

GRAPHICAL ABSTRACT

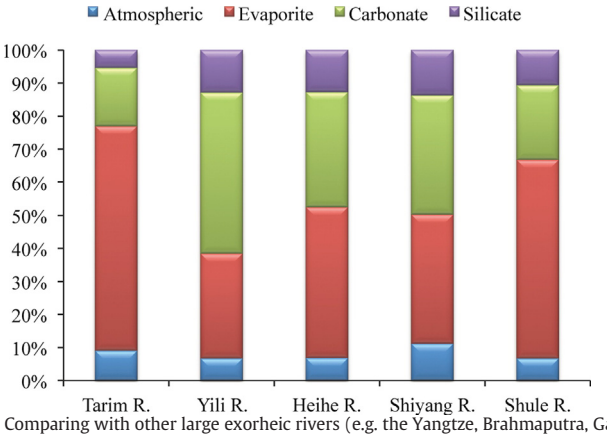

Comparing with other large exorheic rivers (e.g. the Yangtze, Brahmaputra, Ganges), the inland rivers in the northern and northeastern Tibetan Plateau have evidently different chemical weathering features. The average contribution from evaporite dissolution is over 50%, and silicate weathering is relatively weak.

ARTICLE INFO

Article history:
Received 19 June 2015
Received in revised form 31 August 2015
Accepted 12 September 2015
Available online xxxx

Editor: D. Barcelo

Keywords:
Northern and northeastern Tibetan plateau
Inland rivers
Hydrochemistry
Chemical weathering rates

ABSTRACT

The geographic region around the northern and northeastern Tibetan Plateau is the source of several inland rivers (e.g. Tarim River) of worldwide importance that are generated in the surrounding mountains systems of Tianshan, Pamir, Karakorum, and Qilian. To characterize chemical weathering and atmospheric CO_2 consumption in these regions, water samples from the Tarim, Yili, Heihe, Shule, and Shiyang Rivers were collected and analyzed for major ion concentrations. The hydrochemical characteristics of these inland rivers pronouncedly distinguish them from large exorheic rivers (e.g., the Yangtze River and the Yellow River), as reflected in very high total dissolution solids (TDS) values. TDS was 115–4345 mg l^{-1} with an average of 732 mg l^{-1}, which is an order of magnitude higher than the mean value for world rivers (65 mg l^{-1}). The Cheerchen River, Niya River, Keliya River and the terminal lakes of the Tarim River and the Heihe River have TDS values higher than 1 g l^{-1}, indicating saline water that cannot be directly consumed. Therefore, the problem of sufficient and safe drinking water has become increasingly prominent in the northwestern China arid zone. According to an inversion model, the contribution from evaporite dissolution to the dissolved loads in these rivers is 12.5%–99% with an average of 54%. The calculated silicate and carbonate weathering rates are 0.02–4.62 t $km^{-2}y^{-1}$ and 0.01–11.7 t $km^{-2}y^{-1}$ for these rivers. To reduce the influence of lithology, only the silicate weathering rates in different parts of the Tibetan Plateau are compared. A rough variation tendency can be seen in the rates: northern regional (0.15–1.73 t $km^{-2}y^{-1}$) < northeastern regional (0.74–4.62) ≈ western regional (1.75) < eastern regional (0.18–16.4) ≈ southeastern regional (3.5–10.6) < southern regional (13.5–38.0). The weathering

E-mail address: wuwh@nju.edu.cn.

http://dx.doi.org/10.1016/j.scitotenv.2015.09.056

rates did not show a noticeable correlation with a single influencing factor, such as temperature, elevation, vegetation, and physical erosion rates. Rainfall and runoff, however, seems to have a positive correlation with silicate weathering rates.

1. Introduction

The uplift of the Tibetan Plateau was one of the most important geological events in the earth's history, having significant influence on global climate and environment. Some researchers think that the uplifting of plateaus has increased continental chemical weathering of silicate rocks and led to global climate cooling by consuming atmospheric CO_2 throughout the Cenozoic (Raymo et al., 1988; Ruddiman and Kutzbach, 1989; Raymo and Ruddiman, 1992; Ruddiman and Prell, 1997). In recent years, the exorheic rivers originating from the Tibetan Plateau have been widely studied, and these studies showed that these river basins had higher chemical weathering rates than the average of the continent as a whole, exerting important influence on the global carbon cycle and material cycling in oceans (Blum et al., 1998; Harris et al., 1998; Galy and France-Lanord, 1999; Karim and Veizer, 2000; Galy and France-Lanord, 2001; Chen et al., 2002; Bickle et al., 2003; Bickle et al., 2005; Singh et al., 2005; Wu et al., 2005; Hren et al., 2007; Chetelat et al., 2008; Wu et al., 2008a, 2008b; Noh et al., 2009; Li et al., 2014a, 2014b; Bickle et al., 2015; Chapman et al., 2015; Jiang et al., 2015; Manaka et al., 2015; Zhang et al., 2015).

The above-mentioned studies revealed the characteristics and rates of chemical weathering and its contribution to atmospheric CO_2 consumption in the southern, western, and eastern regions of the Tibetan Plateau. In contrast, there are few studies in the vast northern and northeastern portions of the Tibetan Plateau owing to a lack of large exorheic rivers. However, inland rivers in these areas are the main pathways for transport of eroded materials from plateau to inland, and they record important information on uplift and erosion in the northern Tibetan Plateau. Moreover, lakes and inland rivers also provide significant contributions to the global carbon cycle (Meybeck, 1993). The Tarim River is the largest inland river in China and the fifth largest worldwide. The Yili River has the most abundant water discharge of any inland river in China. The Heihe, Shule, and Shiyang Rivers are important water source in the arid zone of Northwest China. These inland rivers have significant effects on the local economy, life, and ecology, both in the extremely arid desert and in the natural grassland. Recently, studies on these rivers have mainly focused on water resource utilization and groundwater remediation and management (Zhang et al., 1995; Feng et al., 2004; Zhu and Yang, 2007; Zhu et al., 2008; Yang et al., 2011; Zhu et al., 2011; Xiao et al., 2012; Zhu et al., 2012; Li et al., 2013). Therefore, systematic hydrochemical studies on these inland rivers are necessary in order to understand the chemical weathering characteristics in different regions of the Tibetan Plateau and to assess their influence on the environment and ecology of the arid zone of Northwest China.

This paper will focus on the hydrochemistry of the inland rivers in the northern and northeastern Tibetan Plateau. The major purposes of this study include: (1) using the method of mass balance to assess the source of major ions in these rivers; (2) calculating chemical weathering rates in these catchments; and (3) analyzing the weathering characteristics and their controlling factors, then assessing the general features of chemical weathering in the whole Tibetan Plateau by comparing with exorheic rivers in other regions.

2. River settings

The Tarim River is the largest inland river in China, and its headwaters are divided into the Akesu River, Yeerqiang River, and Hetian River (Fig. 1; Tables 1 and 2). The Tarim River has a total length of 2137 km and a drainage area of 194,000 km^2. The Yili River originates from the northern Khan Tengri Peak and has a length of 1236 km and a drainage area of 151,000 km^2. It has three headwaters: the Tekesi River, Gongnaisi River, and Kashi River (Fig. 1, Tables 1 and 2).

The Heihe River is located in E96°42′–102°00′, N37°41′–42°42′ and is the second largest inland river in China. It originates from the northern Qilian Mountain and has a length of 918 km and a drainage area of 116,000 km^2 (Fig. 1, Tables 1 and 2). The Shule River is located in E92°11′–98°30′, N38°00′–42°48′, rising from Heliling Glacier in the Qilian Mountain (elevation 5174 m) with a length of 670 km and a drainage area of 41,300 km^2. The Shiyang River is located in E101°41′–104°16′, N36°29′–39°27′ and originates from the northern Qilian Mountains with a length of 300 km and a drainage area of 41,600 km^2.

The geographical and hydrological features are listed in Tables 1 and 2. Geologically, the source areas and catchments of the upper reaches of these inland rivers are covered with Precambrian high-grade metamorphic rocks, Paleozoic volcanic rocks, carbonate rocks, and clastic rocks and granitoids of different stages. Quaternary deposits are widely distributed in the catchments of the middle and lower reaches (Fig. 2).

3. Sampling and analytical methods

24 river water samples from the Tarim River and Yili River were collected in July 2012 (in the high-water stage–wet season, May to September). 27 river water, 1 rainwater, and 2 snow samples from the Heihe, Shule, and Shiyang Rivers were collected in October 2011 (close to high-water stage, May to September). All samples were collected at the riverbank (approximately 10 cm depth from the river surface) and stored in pre-cleaned polyethylene bottles. Water samples were filtered through 0.45 μm Millipore filters. An aliquot of the filtered water was acidified with ultrapure-grade nitric acid (Galy and France-Lanord, 1999). Ca^{2+}, Mg^{2+}, Na^{+}, K^{+}, and Si were measured in filtered and acidified water using ICP-AES (Jarrell-Ash1100) at the Center of Modern Analysis of Nanjing University. The anions (Cl^{-}, NO_3^{-}, and SO_4^{2-}) in filtered and unacidified samples were measured using an ion chromatograph (Dionex series 1100) at the Key Laboratory of Surficial Geochemistry, Ministry of Education, School of Earth Sciences and Engineering, Nanjing University. A portable Digital Titrator (Hach 16,900) was used to measure alkalinity in unfiltered water samples. Total suspended solid (TSS) concentrations were estimated by weighing the material collected on the filter membranes. The measurement reproducibility was determined by repeat analysis of samples and standards, which showed ±2% precision for the cations and ±5% for the anions.

4. Results

4.1. Major ions

The concentrations of total dissolved solids (TDS) of these inland river systems were 115–4642 mg l^{-1} with an average of 674 mg^{-1} (Table 3), an order of magnitude higher than the mean value for world rivers (65 mg l^{-1}) (Meybeck and Helmer, 1989). The terminal lake (the lake that an inland river eventually flows into) (Juyan Lake, sampling number HH10) of the Heihe River has the highest value, which is indicative of a saline lake. TDS in Taitema Lake (TH16), the Kongque River (TH20), the Hetian River (TH6), the Keliya River (TH3), the Cheerchen River (TH1), and the lower Shule River (SLH3) were greater than 1 g^{-1}, indicating brackish water. TDS in the other samples are lower than 1 g l^{-1} still classified as fresh water. The Yili River,

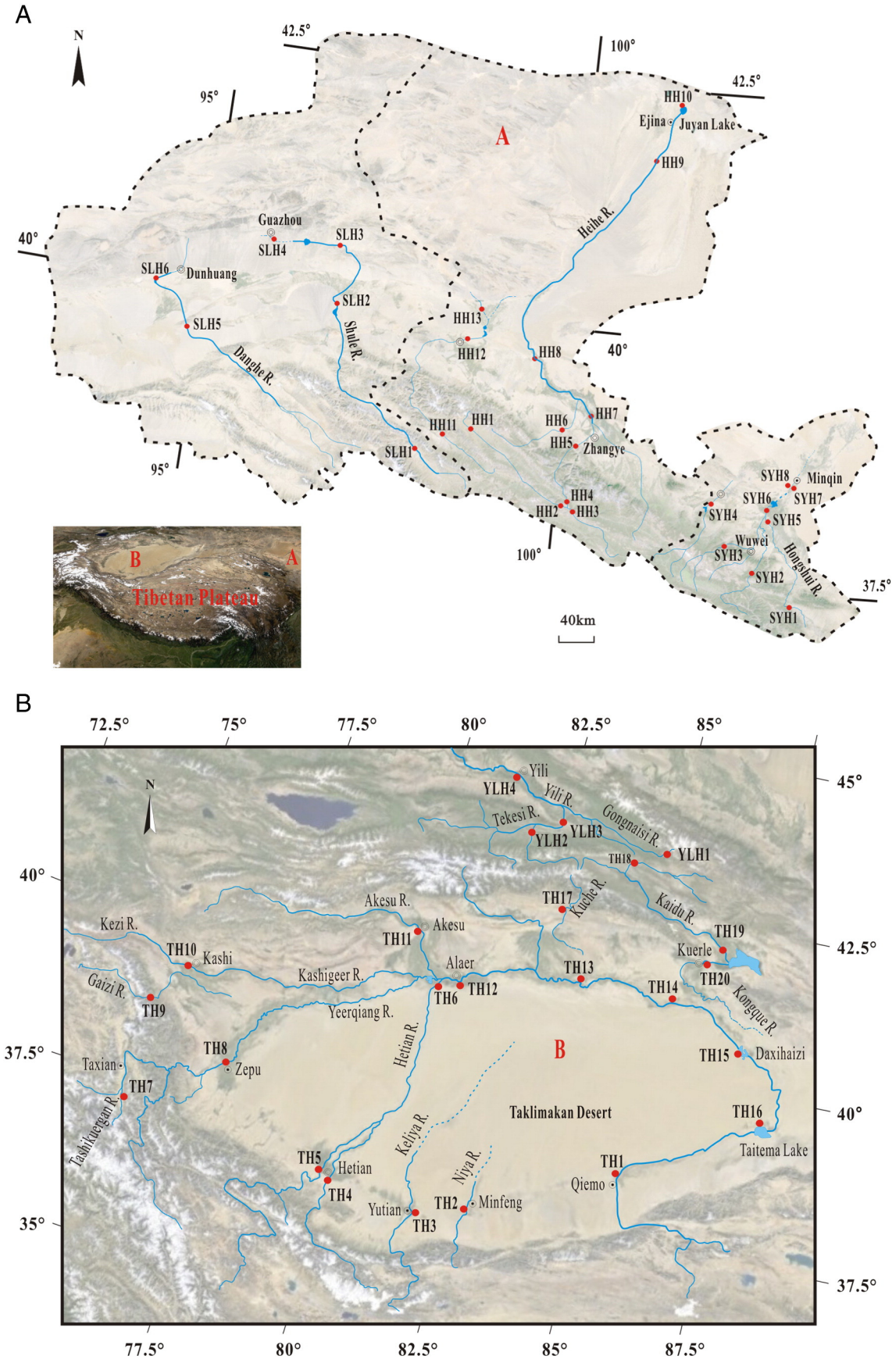

Fig. 1. The map of the inland rivers in the northern and northeastern Tibetan Plateau and sampling locations (filled red circles) (modified from NASG, 2006). (A) The Heihe, Shule, and Shiyang river catchments. (B) The Tarim and Yili river catchments.

Table 1
The geographic and hydrological features of these inland rivers.

River basin	Sub-basin	River length (km)	Drainage area (km^2)	Discharge (km^3)	Temperature (°C)	Annual rainfall (mm)	Annual evaporation (mm)
		2137	194,000		10.6–11.5	17.4–42.8	1125–1600
	Yeerqiang River	1079	50,248	6.57	10.6–11.5	30–60	2400
	Aksu River	530	43,000	7.62	9.2–11.5	64	1890
Tarim River[a]	Hetian River	1090	49,000	4.38	12.2	35.6	2159–3137
	Keliya River	438	3950	0.722	9.53	123	1840
	Cheerchen River	813	48,600	0.8	10.2–10.8	24.5–27.5	2507
	Kaidu River	560	26,300	2.5	6.5–11.5	70–600	500–1500
Yili River[b]		1236	151,000	11.7	2.9–8.4	300	500–1000
		918	116,000				
Heihe River[c]	Upper reaches	303	10,000	1.605	<2	350	
	Middle reaches	204	25,600	1.005	6–8	140	1410
	Lower reaches	411	80,400		8–10	47	2250
Shule River[c]		670	41,300	1.513	6.9–8.8	<50–400	2897–3042
Shiyang River[c]		300	41,600	1.575	0– > 8	<150–650	720–2640

[a] Xijiang Tarim River Basin Management Bureau, 2003.
[b] Kadeer, 1982.
[c] Hydrology and Water Resources Bureau of Gansu Province, 2012.

originating in the northern Tianshan Mountains, has TDS values from 154 to 303 mg l^{-1}, far lower than the other inland rivers.

The total cation charge TZ^+ ($TZ^+ = 2Ca^{2+} + 2Mg^{2+} + Na^+ + K^+$) is 1400–71,345 μeq with an average of 9720 μeq. The total anion charge TZ^- ($TZ^- = Cl^- + HCO_3^- + NO_3^- + 2SO_4^{2-}$) is 1537–76,594 μeq with an average of 10,230 μeq. The normalized inorganic charge balance ($NICB = (TZ^+ - TZ^-) / (TZ^+ + TZ^-)$) is within ±5% for most of the samples, but the Keliya River reaches up to −12%. The relationship between ($Ca^{2+} + Mg^{2+}$) and HCO_3^- drastically deviates from the 1:1 line. In contrast, there is a strongly positive correlation ($r^2 = 0.90$, $n = 51$) between ($Ca^{2+} + Mg^{2+}$) and ($HCO_3^- + SO_4^{2-}$), indicating that evaporites are a significant source of major ions in these rivers (Fig. 3).

4.2. Rain chemistry

Among the three samples of rain and snow waters, the snow sample from the headwater of the Heihe River has relatively high major ion concentration (TDS is 74 mg l^{-1}. Ca^{2+}:308 μmol l^{-1}, Na^+:169 μmol l^{-1}, HCO_3^-:705 μmol l^{-1}, Cl^-:121 μmol l^{-1}). Because there is cement processing equipment for rebuilding the nearby road, high ion concentrations may reflect the contribution of dust deposition. The major ion concentrations of the snow sample from the source area of the Shule River are low, and TDS is only 20 mg l^{-1}. Most of major ion concentrations in the rainwater from Wuwei City are low as well (TDS is 34 mg l^{-1}), but SO_4^{2-} concentration (134 μmol l^{-1}) is noticeably higher than other two snow samples, indicating that the rainwater collected in the city is influenced by acid deposition from industrial activities.

5. Discussion

5.1. The sources of major ions

The major sources of the dissolved load in rivers include: anthropogenic activities (industrial, agricultural, and urban/domestic), rock weathering, atmospheric input, and groundwater/hydrothermal fluids. The upstream areas of these inland rivers are not affected by industrial and agricultural activities and are far away from densely populated areas. The middle and lower reaches of these rivers flow into the desert zone, and influence from anthropogenic activities is not remarkable there either. Therefore, direct anthropogenic contributions to the major ion budgets of these rivers are small and we assume them to be negligible. Moreover, the contribution to the river budgets from deeper water masses (e.g., groundwater) is not taken into account.

5.1.1. Atmospheric input

One of the main sources of major ions, especially of dust precipitation and sea salt, is atmospheric input. As the study area and its river systems are far away from oceans, sea salt input essentially plays no role. In contrast, dust input derived from dust storms represents a major component in the arid region and is much more important. This assumption is also supported by studies by Feng et al. (2004) and Zhu et al. (2008). Assessments of the salinity of rainwater show a pronounced increasing trend from the mountainous source areas to forelands with desert plains. Furthermore, eolian processes from frequent and serious desert storm events kick up saline material (saltation, reptation). The results are high concentrations of major ions in precipitation, and TDS can even reach maxima up to 1000 mg l^{-1} (Feng et al., 2004; Ma et al., 2012). Moreover, the mobilization of materials from adjacent dried saline lakes may also have an important influence on the river waters.

For the Heihe, Shule, and Shiyang Rivers, we use the analyzed values of two snow samples and one rainwater sample combined with data from other researchers (Feng et al., 2004; Zhu et al., 2008; Ma et al., 2012), to evaluate the contribution from atmospheric input. Due to the lack of rainwater samples from the catchments of the Tarim and Yili Rivers, we use data from Urumqi City and Muztagh Ata (snow from glaciers) (Sun et al., 2002; Xu et al., 2008; Zhao et al., 2008; Wang and Xu, 2009). The main factors influencing the chemistry of precipitation are: local Asian dust, material from local sources, acid pollution components, and ocean (or saline lake) material.

5.1.2. Evaporite dissolution

Evaporite dissolution is an important source for the chemical composition of dissolved load in these inland rivers. There is an extremely strong positive correlation between Na and Cl ($r^2 = 0.998$, $n = 51$, Fig. 4a), and samples almost cluster along the 1:1 line. As the elevation of surrounding mountain chains blocks maritime air mass and thus influence from sea salt is weak, halite dissolution must be a dominant source of Na and Cl in the rivers. For those 'normal' rivers having Na and Cl concentrations lower than 500 μmol l^{-1}, Na exceeds Cl (Fig. 4b). This is evidence of silicate weathering from metamorphic and magmatic series as a further main source of Na. Apparently, K and Cl show good correlation in these samples ($r^2 = 0.946$, $n = 51$, Fig. 4c). When samples with low values of K and Cl are plotted, however, the correlation becomes weak ($r^2 = 0.39$, $n = 19$) (Fig. 4d). Contribution from sylvite deposits (KCl) is relatively important only in the two terminal lakes (Taitema Lake, TH16, and Juyan Lake, HH10). Although the correlation coefficient between SO_4 and Na reaches 0.898 ($n = 51$, Fig. 5a, b), there is no strong correlation ($r^2 = 0.48$, $n = 47$) after

Table 2
Sampling details of these inland rivers.

Sampling numbers	River basins	Date	Locations	Longitude	Latitude	Elevation (m)
The Heihe River						
HH1	Heihe River	31-Oct.-11	Yeliugou	98°52′54.9″	38°50′49.9″	3782
HH2	Heihe River	1-Nov.-11	Qilian	100°10′49.9″	38°13′18.3″	2620
HH3	Babao River	1-Nov.-11	Qilian	100°13′11.6″	38°11′42.5″	2683
HH4	Heihe River	1-Nov.-11	Husitai	100°10′35.7″	38°14′51.2″	2595
HH5	Heihe River	24-Oct.-11	Yingluo Gorge	100°10′12.6″	38°48′12.8″	1698
HH6	Liyuan River	24-Oct.-11	Liyuan	100°00′12.7″	38°58′31.0″	1771
HH7	Heihe River	25-Oct.-11	Jing'an	100°23′56.8″	39°08′05.6″	1420
HH8	Heihe River	25-Oct.-11	Luocheng	99°34′46.1″	39°39′40.7″	1305
HH9	Heihe River	25-Oct.-11	Donghe Bridge	100°59′16.1″	41°48′15.5″	959
HH10	Heihe River	26-Oct.-11	Juyan Lake	101°14′53.5″	42°20′10.6″	907
HH11	Baida River	31-Oct.-11	Yanglong	98°24′23.7″	38°48′46.3″	3362
HH12	Baida River	27-Oct.-11	Jiuquan	98°32′26.2″	39°46′05.7″	1438
HH13	Baida River	27-Oct.-11	Yuanyangchi	98°51′22.4″	40°01′23.0″	1266
	Snow	31-Oct.-11	Tuolainan Mt.	98°52′54.9″	38°50′49.9″	3782
The Shule River						
SLH1	Shule River	31-Oct.-11	Shuli	98° 2′30.4″	38°40′11.4″	3676
SLH2	Shule River	27-Oct.-11	Changmabao	96°47′58.2″	39°59′30.2″	1938
SLH3	Shule River	28-Oct.-11	Hedong	96°45′03.6″	40°33′42.8″	1366
SLH4	Shule River	28-Oct.-11	Guazhou	95°48′43.5″	40°30′22.3″	1183
SLH5	Danghe River	29-Oct.-11	Lucaowan Bridge	94°50′21.2″	39°33′22.8″	2046
SLH6	Danghe River	29-Oct.-11	Danghe reservoir	94°19′40.8″	39°57′12.2″	1437
	Snow	31-Oct.-11	SuleNan Mt.	98°8′19.9″	38°42′54.7″	4321
The Shiyang River						
SYH1	Gulang River	22-Oct.-11	Shibali	102°55′30.8″	37°23′59.2″	2215
SYH2	Zamu River	22-Oct.-11	Gucheng	102°35′00.0″	37°42′43.6″	1973
SYH3	Xiying River	23-Oct.-11	Xiying	102°19′16.5″	37°57′32.2″	1877
SYH4	Xida River	24-Oct.-11	Hexibao	102°00′37.8″	38°19′59.3″	1855
SYH5	Hongshui River	23-Oct.-11	Caiqi	102°45′30.7″	38°10′27.7″	1451
SYH6	Shiyang River	23-Oct.-11	Caiqi	102°45′13.4″	38°12′57.9″	1444
SYH7	Daxi River	23-Oct.-11	Minqin	103°03′49.7″	38°33′39.9″	1378
SYH8	Dadong River	23-Oct.-11	Minqin	103°03′52.7″	38°33′39.1″	1378
	Rain	23-Oct.-11	Wuwei	102°38′29.2″	37°55′41.2″	1537
The Tarim River						
TH1	Cheerchen River	15-Jul.-12	Qiemo	85°30′54.3″	38°12′38.6″	1214
TH2	Niya River	15-Jul.-12	Minfeng	82°39′13.0″	36°55′13.0″	1639
TH3	Keliya River	16-Jul.-12	Yutian	81°42′15.1″	36°51′49.9″	1397
TH4	Yulongkashi River	16-Jul.-12	Hetian	79°57′24.9″	37°06′33.0″	1369
TH5	Kalakashi River	17-Jul.-12	Hetian	79°45′37.1″	37°15′17.4″	1313
TH6	Hetian River	20-Jul.-12	Alaer	80°53′26.2″	40°25′11.7″	1028
TH7	Tashikuergan River	18-Jul.-12	Taxian	75°28′19.5″	37°08′40.8″	3719
TH8	Yeerqiang River	17-Jul.-12	Zepu	77°16′25.8″	38°15′11.9″	1249
TH9	Gaizi River	19-Jul.-12	Gaizi Gorge	75°24′11.5″	38°48′54.3″	2161
TH10	Kezi River	18-Jul.-12	Kashi	75°55′30.8″	39°27′13.7″	1294
TH11	Akesu River	21-Jul.-12	Akesu	80°13′17.1″	41°07′11.0″	1098
TH12	Mainstream	21-Jul.-12	Alaer	81°17′51.6″	40°32′01.8″	1011
TH13	Mainstream	22-Jul.-12	Luntai	83°41′27.4″	41°00′52.7″	947
TH14	Mainstream	14-Jul.-12	Yuli	85°46′22.3″	41°05′22.8″	899
TH15	Mainstream	14-Jul.-12	Daxi Lake	87°33′27.4″	40°35′25.4″	855
TH16	Mainstream	14-Jul.-12	Taitema Lake	88°17′04.5″	39°29′04.4″	809
TH17	Kuche River	23-Jul.-12	Kuche	83°02′16.4″	42°04′47.7″	1466
TH18	Kaidu River	24-Jul.-12	Bayinbuluke	84°15′18.1″	43°03′25.9″	2464
TH19	Kaidu River	13-Jul.-12	Yanqi	86°25′59.7″	42°07′14.6″	1065
TH20	Kongque River	13-Jul.-12	Keerle	86°11′18.7″	41°47′38.0″	968
The Yili River						
YLH1	Gongnaisi River	24-Jul.-12	Gongnaisi	84°38′08.1″	43°15′07.5″	2049
YLH2	Tekesi River	26-Jul.-12	Tekesi	81°54′07.1″	43°07′37.0″	1231
YLH3	Tekesi River	25-Jul.-12	Gongliu	82°29′07.6″	43°25′14.8″	867
YLH4	Mainstream	27-Jul.-12	Yining	81°15′32.0″	43°53′32.7″	599

removing four high points ($Na > 10{,}000\ \mu mol\ l^{-1}$), showing that contribution from mirabilite ($Na_2SO_4 \cdot 10H_2O$, an evaporite deposit) is only important in several locations (e.g., the Cheerchen River, Hetian River, Taitema Lake, and Juyan Lake) where evaporation is strong. There is a strongly positive correlation between (Ca + Mg) and SO_4 ($r^2 = 0.896$, $n = 51$), which indicates that SO_4 is mainly from evaporite dissolution. The correlation between Mg and SO_4 is better than that between Ca and SO_4 (Fig. 5c, d), showing that the contribution from evaporites to Mg exceeds that to Ca.

5.1.3. Silicate weathering

Silicates are a main contributor when weathering of albite and Ca-plagioclase to kaolinite, of K-feldspar to montmorillonite and finally of olivine weathering takes place. In the source areas and upper reaches of these inland rivers, granite and metamorphic rocks are exposed. The middle and lower reaches flow through Quaternary deposits, which include some silicate compositions as well (China Geological Survey, 2004). Therefore, silicate weathering has a certain contribution to the hydrochemistry. Si concentrations in these rivers are commonly

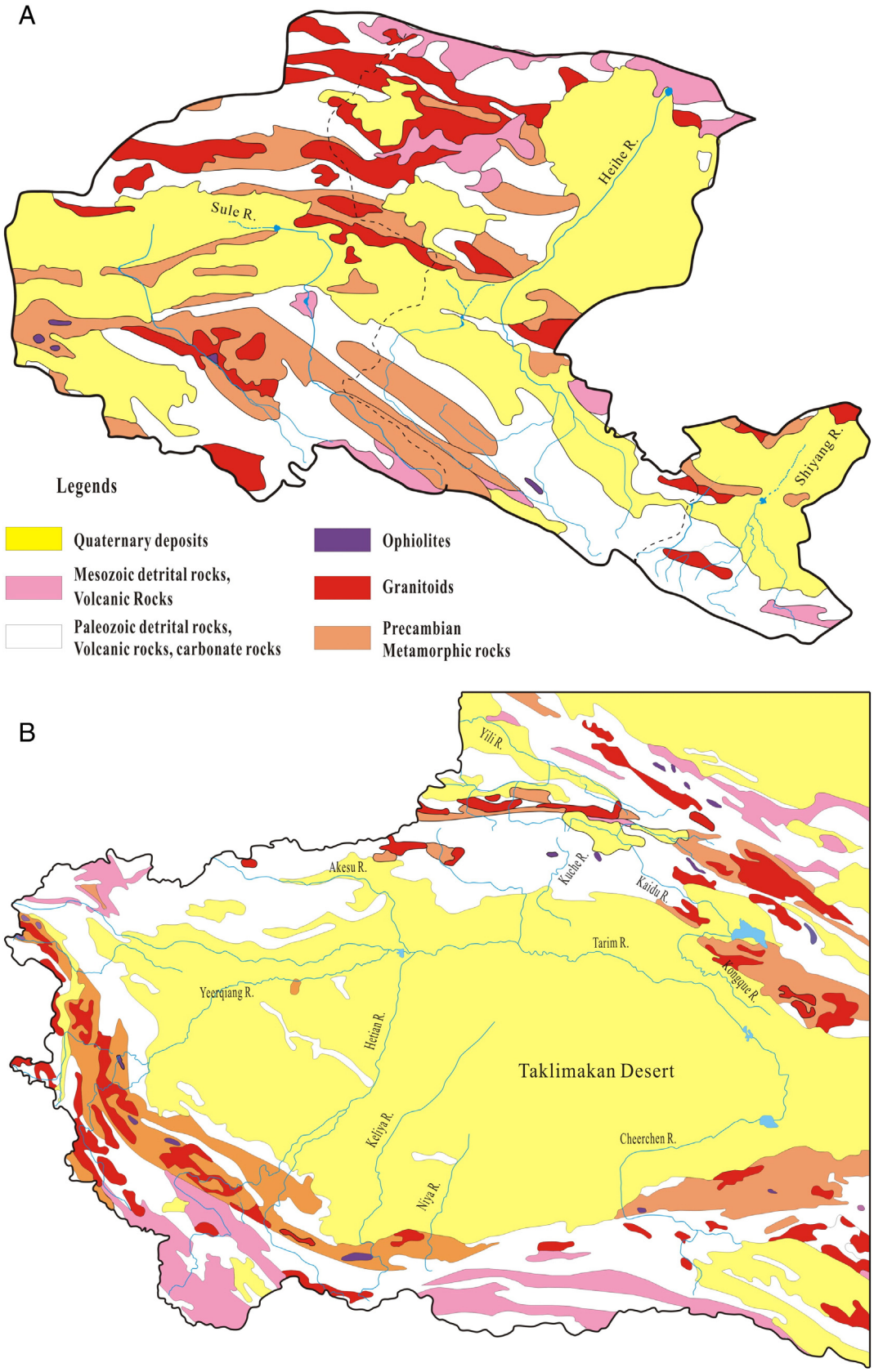

Fig. 2. The geological maps (Modified from China Geological Survey, 2004). (A) The Heihe, Shule, and Shiyang River Catchments. (B) The Tarim and Yili River Catchments.

low, and most of the headwaters and upper reaches do not exceed 100 μmol l^{-1}, reflecting the constraints of the arid and cold climate on chemical weathering. Si concentration in samples TH1 and TH3 are 347 μmol $l^{-1}$and 258 μmol l^{-1}, respectively, which are the highest in the whole catchment. The higher Si concentrations do not derive from more intense silicate weathering. The major ion characteristics show

Table 3
Hydrochemical data of these inland river systems in the Northwest of China.

Number	Drainage area km^2	Discharge $km^3 y^{-1}$	Runoff mm y^{-1}	Ca	Mg	K	Na	Si	HCO_3	Cl	SO_4	NO_3	TDS [a] mg^{-1}	TSS [b] mg^{-1}	TZ^+ [c]	TZ^-	NICB [d]	Hydrological type
				$\mu mol\ l^{-1}$											μeq	μeq		
The Shiyang River																		
SYH1	877	0.078	88.5	1694	1031	80.5	931	120	4380	428	999	64.3	500	8.15	6461	6869	−3.1	Ca > Mg > Na, HCO_3 > SO_4 > Cl
SYH2	851	0.254	298	1582	597	44.9	402	84.6	3110	150	1002	61.2	384	7.92	4804	5325	−5.1	
SYH3	1455	0.382	263	1957	808	40.8	367	96.8	2980	154	1401	56.6	433	3.96	5937	5992	−0.5	
SYH4	2053	0.122	59.4	1534	850	52.3	921	93.2	3260	452	1142	0.0	430	2.58	5742	5995	−2.2	Ca > Na > Mg, HCO_3 > SO_4 > Cl
SYH5	3361	0.140	41.7	1449	887	69.2	1731	121	3670	1279	954	0.0	483	752	6471	6857	−2.9	Na > Ca > Mg, HCO_3 > Cl > SO_4
SYH6	10,209	0.166	16.3	1440	891	69.0	1667	127	3760	1167	889	44.8	476	699	6397	6750	−2.7	
SYH7				1316	861	86.7	1244	96.1	2980	774	1112	36.4	422	44.1	5685	6015	−2.8	Ca > Na > Mg, HCO_3 > SO_4 > Cl
SYH8				1346	861	86.4	1198	95.0	2920	736	1008	0.0	407	40.8	5697	5671	0.2	
				132	39	27.4	87	13.9	130	53	134	27.4	34		457	479	−2.3	
The Heihe River																		
HH1				1654	881	44.1	825	83.6	3740	660	750	63.9	436	5.88	5940	5964	−0.2	Ca > Mg > Na, HCO_3 > SO_4 > Cl
HH2	2452	0.438	179	2144	1369	74.1	1193	125	4710	282	1666	57.1	610	70.4	8292	8381	−0.5	
HH3	4589	0.706	154	1833	1347	66.7	883	139	4190	204	1257	50.0	516	87.8	7309	6957	2.5	
HH4				1848	1339	67.9	865	132	4200	224	1444	66.8	536	79.5	7308	7379	−0.5	
HH5	10,009	1.59	158	1712	1330	67.9	883	118	3890	315	1412	80.4	513	21.2	7034	7109	−0.5	
HH6	2240	0.248	111	1565	1128	56.2	904	91.8	3490	329	1009	77.0	439	27.0	6347	5914	3.5	
HH7	20,299	1.03	50.9	1489	1476	119	1664	187	4440	795	1226	96.8	561	2.69	7713	7785	−0.5	Na > Ca > Mg, HCO_3 > SO_4 > Cl
HH8	35,634	1.04	29.2	1636	1737	116	2458	197	4790	1313	1896	82.1	695	54.3	9318	9977	−3.4	Na > Mg > Ca, HCO_3 > SO_4 > Cl
HH9		0.603		1384	2007	120	2689	187	4090	1248	2041	118	668	221	9590	9539	0.3	
HH10	116,000	0.322	2.77	1380	11,996	1610	37,609	72.1	4410	29,332	21,411	29.5	4642	0.500	65,971	76,594	−7.5	Na > Mg > Ca, Cl > SO_4 > HCO_3
HH11				1520	648	49.2	363	120	3350	212	444	55.3	345	11.7	4749	4506	2.6	Ca > Mg > Na, HCO_3 > SO_4 > Cl
HH12	7095	0.646	91.1	1230	1306	76.2	554	139	3800	354	945	52.4	435	196	5701	6096	−3.3	Mg > Ca > Na, HCO_3 > SO_4 > Cl
HH13	12,439			1301	1642	149	1092	94.6	3690	652	1784	44.4	545	7.65	7126	7954	−5.5	
				308	47.7	68.5	169	17.1	705	121	41	36.3	74		949	944	0.2	
The Shule River																		
SLH1	10,961	0.894	81.6	1223	1067	44.6	1693	129	4570	1183	643	0.0	498	91.3	6317	7040	−5.4	Na > Ca > Mg, HCO_3 > Cl > SO_4
SLH2	18,496	0.280	15.1	1175	1277	62.8	1224	114	3440	880	1091	0.0	454	4.73	6191	6502	−2.5	Mg > Na > Ca, HCO_3 > SO_4 > Cl
SLH3				2108	3786	149	6026	199	4590	4795	4652	0.0	1218	1.62	17,964	18,689	−2.0	Na > Mg > Ca, Cl > SO_4 > HCO_3
SLH4	14,325	0.353	24.6	1220	1522	96.7	1783	116	3120	1324	1737	0.0	535	12.8	7363	7918	−3.6	Na > Mg > Ca, HCO_3 > SO_4 > Cl
SLH5	16,970	0.299	17.6	1777	2532	157	5365	215	4400	4294	2965	97.9	974	0.364	14,140	14,722	−2.0	Na > Mg > Ca, HCO_3 > Cl > SO_4

SLH6				1144	1325	89.5	2082	154	3710	1637	1125	67.3	526	6.35	7108	7664	−3.8	
				48.8	17.7	28.2	103	4.64	135	84.7	27.3	0	20		265	274	−1.8	
The Tarim River																		
TH1	24,692	0.524	21.2	2950	3663	851	15,304	347	2115	16,305	6027	267	1895	3606	29,381	30,740	−2.3	$Na > Mg > Ca, Cl > SO_4 > HCO_3$
TH2	1734	0.165	95.2	2940	896	136	1844	115	1049	1800	3983	92.6	703	2695	9652	10,907	−6.1	$Ca > Na > Mg, SO_4 > Cl > HCO_3$
TH3	7358	0.722	98.1	914	1364	490	7913	258	3836	8030	2207	186	1013	3.49	12,959	16,466	−11.9	$Na > Mg > Ca, Cl > HCO_3 > SO_4$
TH4	14,575	2.31	158	1122	466	121	1894	90.6	1500	1645	922	84.1	348	616	5190	5072	1.1	$Na > Ca > Mg, Cl > HCO_3 > SO_4$
TH5	19,983	2.19	110	1165	447	113	1914	79.3	1475	2148	975	57.8	369	641	5252	5632	−3.5	
TH6	48,870	0.915	18.7	2653	3178	478	19,222	149	1672	18,482	6370	124	2021	2000	31,362	33,019	−2.6	$Na > Mg > Ca, Cl > SO_4 > HCO_3$
TH7	7780	1.13	145	535	110	23.5	85.6	47.4	1148	48	149	33.6	115	20.5	1400	1528	−4.4	$Ca > Mg > Na, HCO_3 > SO_4 > Cl$
TH8	50,248	6.57	131	1204	440	118	929	98.0	1410	907	1013	62.9	304	2741	4335	4405	−0.8	$Ca > Na > Mg, HCO_3 > SO_4 > Cl$
TH9	9753	0.948	97	958	290	80.7	456	111	1426	226	792	72.4	235	944	3031	3309	−4.4	$Ca > Mg > Na, HCO_3 > SO_4 > Cl$
TH10	13,700	2.14	156	3665	981	97.9	1707	131	1213	1638	4297	69.8	763	1303	11,098	11,514	−1.8	$Ca > Na > Mg, SO_4 > Cl > HCO_3$
TH11	43,123	7.62	177	1039	484	69.2	276	73.9	1434	210	719	49.9	229	1418	3391	3132	4.0	$Ca > Mg > Na, HCO_3 > SO_4 > Cl$
TH12	266,200	4.57	17.2	1327	990	150	3624	102	1557	3803	1507	132	549	1849	8408	8506	−0.6	$Na > Ca > Mg, Cl > HCO_3 > SO_4$
TH13		3.75		1185	1065	164	4132	99.0	1361	4201	1834	30.2	585	153	8797	9259	−2.6	$Na > Ca > Mg, Cl > SO_4 > HCO_3$
TH14		2.85		1233	1103	166	3381	137	1590	3299	1982	44.3	567	2344	8218	8898	−4.0	
TH15		0.550		1502	1510	225	5018	138	1508	5161	2936	23.9	780	11.6	11,268	12,566	−5.4	$Na > Mg > Ca, Cl > SO_4 > HCO_3$
TH16				8113	6914	1679	39,613	179	1492	39,097	14,562		4345	0.872	71,345	69,714	1.2	$Na > Ca > Mg, Cl > SO_4 > HCO_3$
TH17	3118	0.374	120	1390	622	133	973	112	1721	1035	1239	116	366	6307	5130	5349	−2.1	$Ca > Na > Mg, HCO_3 > SO_4 > Cl$
TH18	18,827	3.50	186	1054	522	32.0	382	128	2377	284	317	35.6	253	72.2	3567	3331	3.4	$Ca > Mg > Na, HCO_3 > SO_4 > Cl$
TH19	22,516	2.60	115	1141	489	42.7	356	106	2328	232	405	36.8	259	30.7	3657	3407	3.5	
TH20				1312	2417	274	7170	81.0	2672	6202	3574	16.0	1014	21.2	14,901	16,038	−3.7	$Na > Mg > Ca, Cl > SO_4 > HCO_3$
The Yili River																		
YLH1	3532	1.44	407	849	147	17.2	134	101	918	58	533	53.8	154	41.0	2142	2096	1.1	$Ca > Mg > Na, HCO_3 > SO_4 > Cl$
YLH2	5666	2.15	379	987	415	32.8	225	58.4	1459	197	627	76.2	217	950	3063	2986	1.3	
YLH3	27,402	7.86	287	873	308	38.1	250	78.1	1361	142	437	66.8	184	7.18	2649	2442	4.1	
YLH4	61,640	15.9	257	1137	509	55.8	972	90.1	1820	556	902	48.5	303	57.8	4319	4229	1.1	$Ca > Na > Mg, HCO_3 > SO_4 > Cl$

[a] TDS: the total dissolved solid.
[b] The total suspended solid.
[c] TZ: total ion charge.
[d] NICB: the normalized inorganic charge balance, $NICB = (TZ^+ - TZ^-) / (TZ^+ + TZ^-)$.

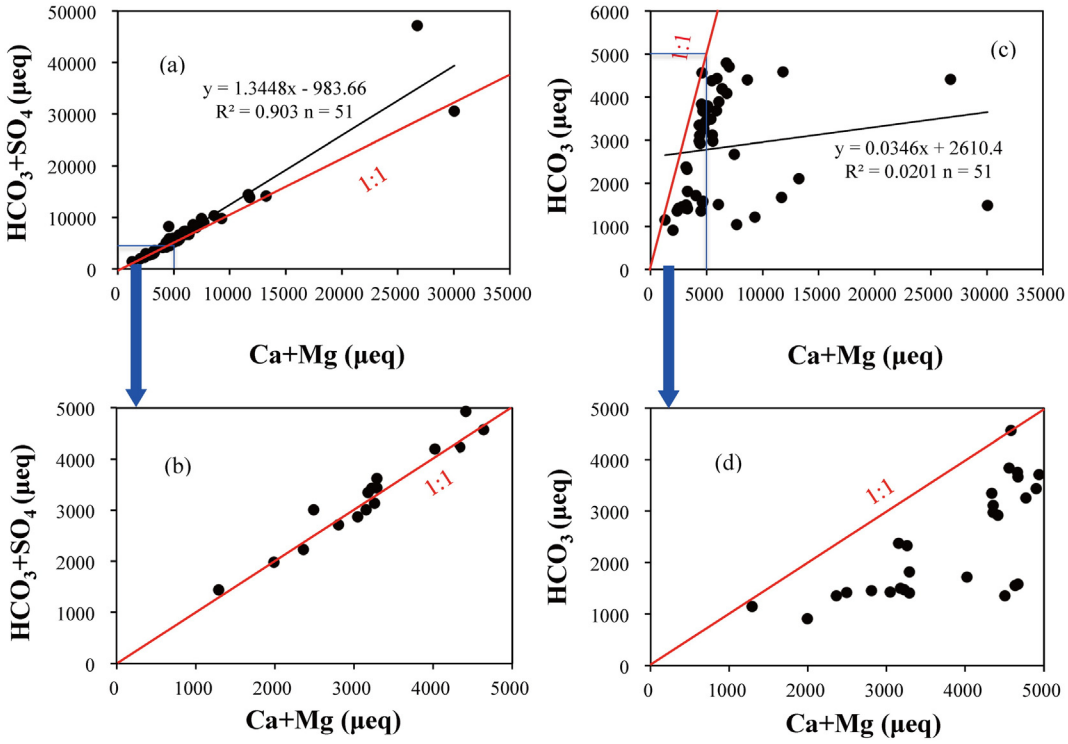

Fig. 3. Scatter plots of (Ca + Mg) versus (HCO_3 + SO_4) (a, b) and HCO_3 (c, d) in these inland rivers. There is strongly positive correlation between (Ca + Mg) and (HCO_3 + SO_4) which also clusters to 1:1 line, indicating that evaporite is an important source of the dissolved loads in rivers.

that the two rivers are typically dominated by evaporite dissolution, and Si is abundantly enriched. However, the terminal lake (Taitema Lake, TH16) of the Tarim River, which has the most evaporation (TDS > 4 g l^{-1}, 1, 2 times of the Cheerchen River, and 4 times of the Keliya River), has a low Si concentration of 179 μmol l^{-1}. It may be attributed to Si uptake from diatoms in lentic lakes, or that the two high Si concentrations may derive from contribution from hydrothermal input. A weak correlation ($r^2 = 0.206$, $n = 51$) between Si and $(Na + K)_{sil}$ (that is, from silicate weathering) indicates that Si in these inland rivers is not entirely from silicate weathering (Fig. 6).

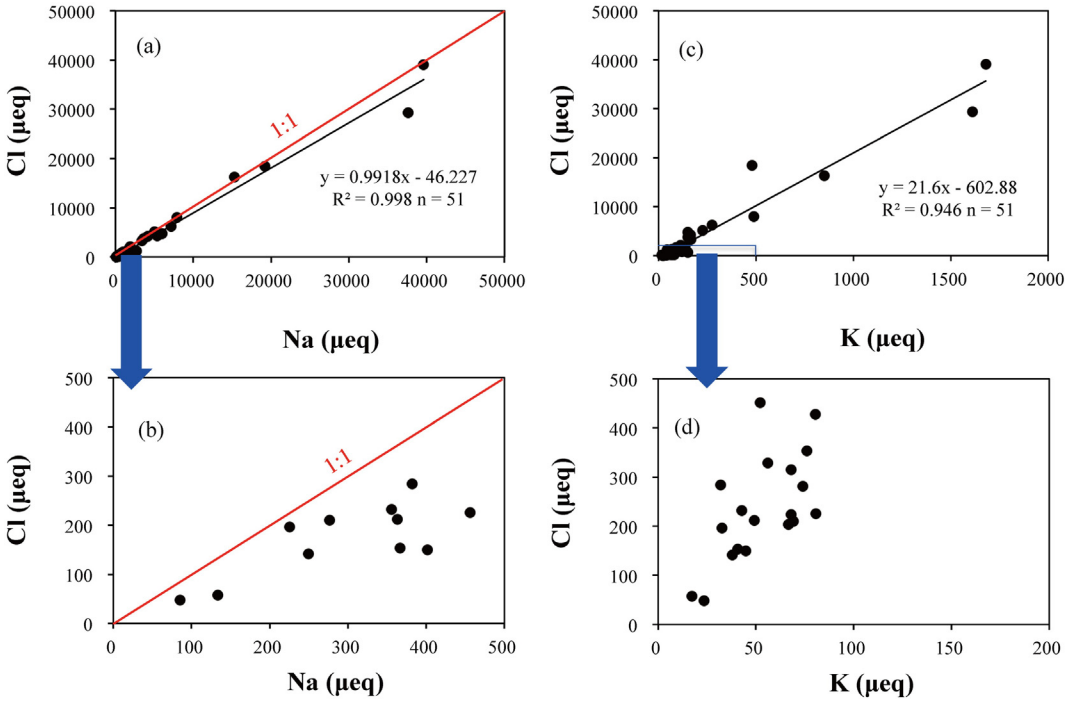

Fig. 4. Scatter plots of Cl versus Na (a, b) and K (c, d) in these inland rivers. There is excellent correlation between Cl and Na, and it seems overlaps the 1:1 line, showing the contribution from halite. For those sample points with low concentrations of Na and Cl, Na exceeds Cl, indicating the contribution from other sources, mainly silicate weathering (b).

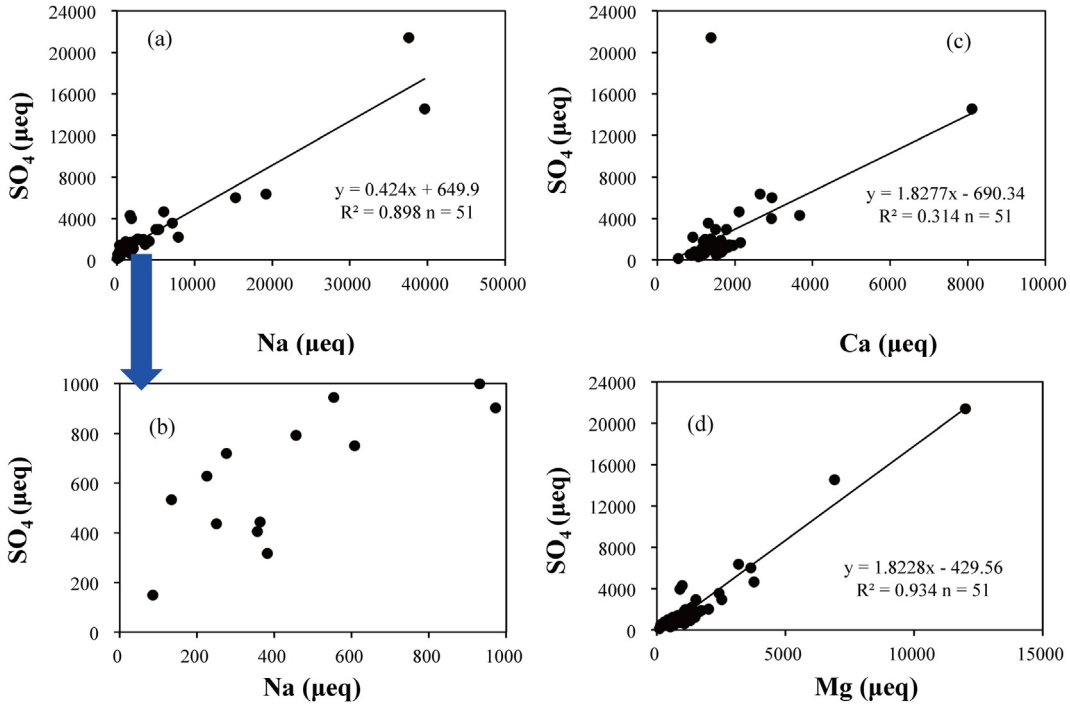

Fig. 5. Scatter plots of SO_4 versus Na (a, b) and Ca (c) and Mg (d) in these inland rivers. High values mainly due to evaporite dissolution.

5.1.4. Carbonate weathering

Carbonate rocks are abundantly exposed in the source areas and upper reaches of these inland rivers. In Quaternary deposits in the middle and lower reaches, loess contains some carbonate as well (China Geological Survey, 2004). HCO_3 concentrations in these rivers are pronouncedly higher than those in small silicate catchments (<1000 μmol l^{-1}) (Oliva et al., 2003; Wu et al., 2013) but lower than those in karst rivers (approximately 2000–3000 μmol l^{-1})(Xu and Liu, 2007; Gao et al., 2009; Wang et al., 2012). High Ca and especially Mg concentrations mainly result from evaporite dissolution.

5.2. Contribution from different sources

To identify the above-mentioned source contributions to the major ions, we use an inversion model (Negrel et al., 1993; Gaillardet et al., 1999; Roy et al., 1999; Millot et al., 2003; Wu et al., 2005; Moon et al., 2007; Chetelat et al., 2008; Wu et al., 2013). The model assumes that the chemical composition of the dissolved load in the rivers is the result of a mixing of different sources. The four main sources (end-members) are atmospheric input, silicate weathering, carbonate weathering, and evaporite dissolution. The mass equations are (Negrel et al., 1993; Gaillardet et al., 1999):

$$\left(\frac{x}{Na}\right)_{\text{river}} = \sum_i \left(\frac{x}{Na}\right)_i \alpha_{i,Na} \quad (1)$$

$$\sum_i \alpha_{i,Na} = 1 \quad (2)$$

where x is Ca^{2+}, Mg^{2+}, K^+, and Cl^-, *i* is the different end-members, and $\alpha_{i,Na}$ is proportion of Na^+ in the different sources. Starting from an a priori set of end-member compositions, $(X/Na)_I$ (Table 4), we iteratively solve for the proportion of those four end-members in each sample ($\alpha_{i,Na}$) and the end-member compositions themselves $(X/Na)_i$. The global optimization process within the optimization software package finds the solution that best predicts the measured compositions in the

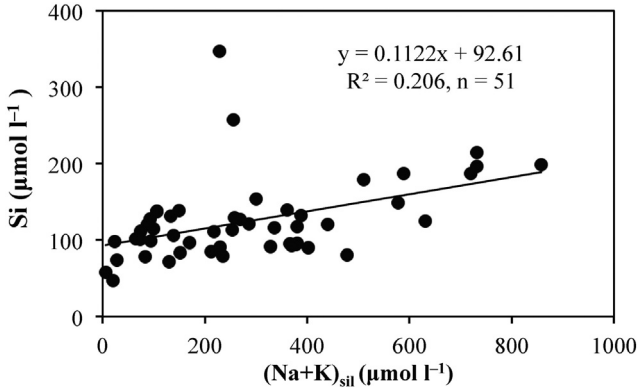

Fig. 6. Scatter plot of Si vs. $(Na + K)_{sil}$. Weak correlation indicates complex Si behavior owing to the predominance of evaporation in these inland rivers.

Table 4
Composition of the different end-members used in our calculation.

End-member	Ca/Na	Mg/Na	K/Na	Cl/Na
The Tarim and Yili River[a]				
Rain	1.77–4.58	0.34–1.46	0.135–0.369	0.63–1.61
Evaporite	0.15–5	0.01–0.5	0–0.2	0.8–1.1
Carbonate	30–70	10–28	0	0
Silicate	0.2–0.5	0.12–0.36	0.01–0.3	0
The Heihe, Shule, and Shiyang Rivers[b]				
Rain	0.47–1.82	0.17–0.45	0.173–0.405	0.61–0.82
Evaporite	0.15–5	0.01–0.5	0–0.2	0.8–1.1
Carbonate	30–70	10–28	0	0
Silicate	0.2–0.5	0.12–0.36	0.01–0.3	0

[a] The rainwater end-member is based on local rain in Urumqi City and Muztagh Ata (Sun et al., 2002; Xu et al., 2008; Zhao et al., 2008; Wang and Xu, 2009); The rock weathering end-members modified from Gaillardet et al. (1999); Wu et al. (2005); Chetelat et al. (2008), and the range of evaporite end-member for these inland rivers is designed wider.
[b] The rainwater end-member is based on our measured values.

least-squares sense. The calculated contributions of different sources to Ca^{2+}, Mg^{2+}, Na^{+}, and K^{+} in the rivers are shown in Fig. 7.

Generally, for the Tarim River, the contribution from evaporite dissolution is low (approximately 20%) in the Kaidu River (TH18–TH19) and the headwater Tashikuergan River of the Yeerqiang River (TH7), and it is close to 50% in Gaizi River and Akesu River (TH9 and TH11), but it reaches 73.3%–95% in the middle and lower reaches of the Tarim River mainstem, Hetian River, Cheerchen River, Keliya River, and Niya River. By contrast, for the Yili River, the contribution from evaporite dissolution is approximately 50% only in the mainstem (TH24), and the contribution from carbonate weathering is more important, reaching 50.8%–61.6%.

For the Heihe, Shule, and Shiyang Rivers, the contribution from evaporites increases remarkably from source areas to the lower reaches because the three rivers ultimately flow into desert. In the headwaters, the Shule River has the highest contribution from evaporite (47.5%), followed by the Heihe River (33.9%), and the tributary Baidahe River is only at 21.5%. Contributions from carbonate weathering in the upper reaches of the Heihe River and the Shiyang River are relatively high. Cambrian carbonate rocks, including intercalated mudrocks and shales, are widely exposed in the upper reaches of the Heihe River, and Paleozoic carbonate rocks and granites are distributed in the upstream Shiyang. As the two rivers flow into desert, rainfall decreases sharply and evaporation becomes strong. Therefore, the contribution from evaporites evidently increases, and the contributions from silicate and carbonate decrease. In the terminal lake of the Heihe River (HH10), the contribution from evaporites is high, up to 99%. The contribution from evaporites in the middle and lower reaches of the Shule River is higher than 50%. In the three inland rivers, the contribution from silicate weathering is relatively low.

5.3. Chemical weathering rates

Silicate weathering rates (SWR) and carbonate weathering rates (CWR) are calculated as follows:

$$SWR = (Ca_{sil} + Mg_{sil} + Na_{sil} + K_{sil}) \times runoff \quad (3)$$

$$CWR = (Ca_{carb} + Mg_{carb}) \times runoff \quad (4)$$

Ca_{sil}, Mg_{sil}, Na_{sil}, and K_{sil} are the concentrations from silicate weathering, and Ca_{carb} and Mg_{carb} are the concentrations from carbonate weathering. As we only have one-time samples, it is crucial whether these samples really reflect the average water chemistry and weathering regimes in the watersheds. The investigation of (Qin et al., 2006) on ttime-series analyses of major ion concentrations at the Min Jiang monitoring station showed that the chemical weathering flux obtained by using major ionic data during water-rich months shows the best agreement with annual time-series estimates ($<\pm 10\%$) and is the worst during the water-lean period (up to 37%). The calculated SWR is 0.05–1.73 t $km^{-2}y^{-1}$ in the Tarim River, and SWR > 1 t $km^{-2}y^{-1}$ is only found in some headwaters and upper reaches just flowing out of mountains. SWR is only 0.05 t $km^{-2}y^{-1}$ in the Tarim River at Alaer City (TH6). Although no SWR is given downstream from Alaer City owing to a lack of data on discharge area, it is conceivable that SWR is lower after flowing into desert with decreasing water discharge. CWR is 0.47–6.52 t $km^{-2}y^{-1}$, and the Kaidu River (TH18) shows maxima. In contrast, chemical weathering rates in the Yili River are higher than those in the Tarim River. SWR is 5.69 t $km^{-2}y^{-1}$ in the Yili River mainstem (YLH4), and the tributary Tekesi River (YLH3) indicates the highest CWR at 7.39 t $km^{-2}y^{-1}$. The calculated SWR is 0.02–4.62 t $km^{-2}y^{-1}$ for the Heihe River. The upper reaches have relatively high SWR (1.49–4.62 t $km^{-2}y^{-1}$; the tributary Babao River has the highest). SWR in the Shiyang and Shule Rivers are 0.19–2.6 t $km^{-2}y^{-1}$ and 0.23–0.90 t $km^{-2}y^{-1}$, respectively. CWR in the Heihe, Shiyang, and Shule Rivers are 0.01–11.7 t $km^{-2}y^{-1}$, 0.78–13.4 t $km^{-2}y^{-1}$, and 0.66–2.49 t $km^{-2}y^{-1}$, respectively.

The relationships between several parameters and SWR are plotted in Fig. 8 to assess the influencing factors on chemical weathering in these inland rivers. Weak correlations are presented for TSS (which can be used as the physical weathering intensity), topography (elevation), and climate (runoff). It is especially interesting to notice the weak relation between SWR and runoff (they are linear in equations 3 and 4). Therefore, the characteristics of chemical weathering in inland rivers are strikingly different from those in exorheic rivers.

5.4. Comparison of weathering rates in the Tibetan Plateau, Tianshan Mountains and Qilian Mountains

There are many factors influencing local chemical weathering rates, such as lithology, climate (rainfall, runoff, and temperature), topography, physical denudation rates, vegetation, etc. The differences in climate and topography are very distinct in the different regions of the Tibetan Plateau and the Tianshan Mountains. We compare rivers originating from these regions in order to discuss the influence of different factors on chemical weathering rates. As the inland rivers in the northern and northeastern Tibetan Plateau are not on an order of magnitude in size with those exorheic rivers in other regions, we discuss only weathering rates instead of fluxes. Moreover, for comparison reliability, chemical weathering rates calculated in high-water stage are selected.

Some studies have shown that lithology plays an important role in chemical weathering, and chemical weathering rates of evaporite rocks ≫ carbonate rocks ≫ silicate rocks (Meybeck, 1987; Gaillardet et al., 1999). Therefore, we listed silicate and carbonate weathering rates in Table 5. These data enable us to better compare silicate weathering rates in the different parts of the Tibetan Plateau.

In Table 5 and Fig. 9, a rough trend in silicate weathering rates in the Tibet Plateau can be seen: northern < northeastern ≈ western < eastern ≈ southeastern < southern. Among the areas, the Brahmaputra basin flowing through the Himalayan Eastern Syntaxis has the highest SWR, which can be attributed to very strong tectonism and extremely abundant precipitation (the annual precipitation can reach up to 4000–6000 mm). Silicate weathering rates in the upper Ganges (Galy and France-Lanord, 1999) are far higher than those in the upper Brahmaputra (Yarlung Tsangpo River) (Hren et al., 2007), as the Yarlung Tsangpo River basin is mainly located in the rain shadow region of the northern Himalaya (the annual precipitation is only 200–400 mm), and the southern Himalaya is much steeper with more abundant rainfall relative to the northern Himalaya. As shown in Fig. 9, there are good correlations between SWR and rainfall ($r^2 = 0.77$), indicating that rainfall is an important controlling factor in silicate weathering. The tendency of weathering rates to be low in northern regions and high in southern regions is compatible with changing trend in rainfall. It is interesting to notice that there is also a good correlation between SWR and runoff ($r^2 = 0.77$) for the Tibetan rivers (including the large exorheic rivers), which is different from those inland rivers with correlation coefficient only of 0.35. It indicates that the controlling factors in silicate weathering rate are more complex in the inland rivers.

Some researchers have studied small monolithologic rivers and concluded that temperature was the most important controlling factor in chemical weathering rates in catchments (White and Blum, 1995; Oliva et al., 2003). However, this effect is not reflected in these rivers in the Tibetan Plateau (Fig. 9), and it also did not show up in the study on 60 large rivers around the world (Gaillardet et al., 1999). Nevertheless, for single river examples, such as the Jinsha River, Yellow River, Mekong River, and Brahmaputra, there is a strong correspondence between weathering rates and temperature, reflecting that arid and cold source areas have low weathering rates (Wu et al., 2005; Hren et al., 2007; Wu et al., 2008a, 2008b). The influence from topography, including different elevation (Fig. 9) and vegetation, is unremarkable. The influence of evaporation is significant

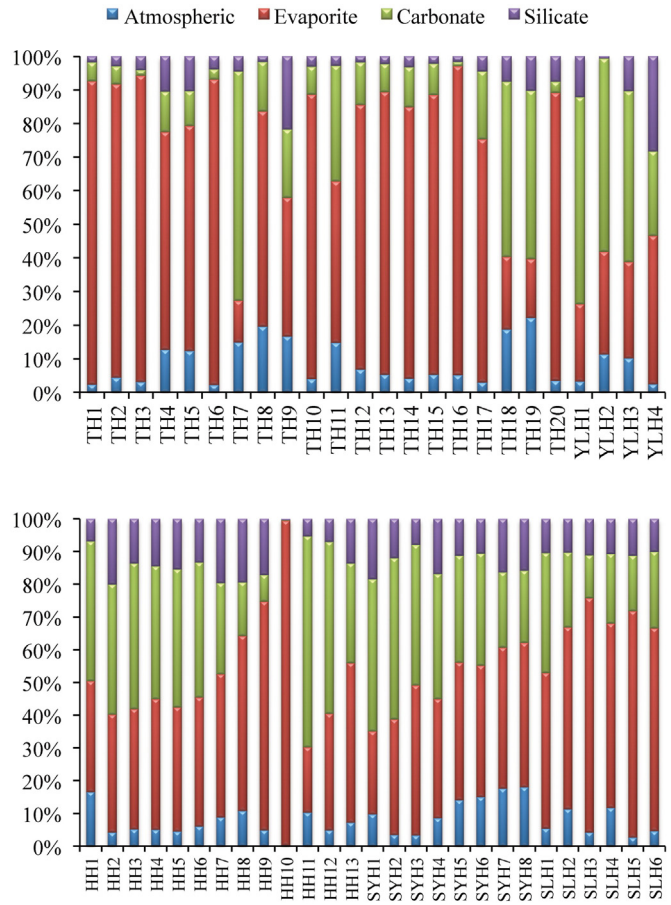

Fig. 7. Diagram showing contribution from the different reservoirs.

only in desert regions with extremely low rainfall, and high evaporation heavily concentrated major ions. These regions are dominated by evaporite dissolution and silicate and carbonate weathering rates are very low.

6. Conclusions

These inland rivers in arid regions in northwestern China show unusual hydrochemical characteristics. The average total dissolved solid (TDS) concentration is high, up to 674 mg l^{-1}, tenfold higher than the mean value of global rivers. Some inland rivers have TDS values much greater than 1 g l^{-1} and cannot be drunk directly, which exacerbates the problems of water resource shortages in these arid regions.

The characteristics of major ion show the dominance of evaporite dissolution. For most of these rivers, the contribution from evaporite is greater than 50%, and it even exceeds 80% in desert regions. Silicate and carbonate weathering are relatively important only in the mountains of the headwaters and upper reaches. Weak correlations between silicate weathering rates (SWR) and TSS, TDS, elevation, and runoff indicate more complex influence from chemical weathering in inland river catchments.

Finally, we compare SWR in different regions of the Tibetan Plateau, Tianshan Mountains, and Qilian Mountains. A total variation tendency is high in the south and low in the north. It does not show great correlation with temperature, runoff, elevation, and vegetation but is generally consistent with the change in rainfall. Chemical weathering rates in the northern Tianshan Mountains are higher than those in the southern part where semi-arid to arid conditions in deserts prevail, which has the lowest weathering intensity after flowing into desert region of the inland rivers originating from the Qilian Mountains.

Acknowledgments

This study was supported by the Natural Science Foundation of China (Project No. 41003001). I thank Wei Xiaochun for his help in the field and all teachers of Nanjing University who helped us for laboratory work.

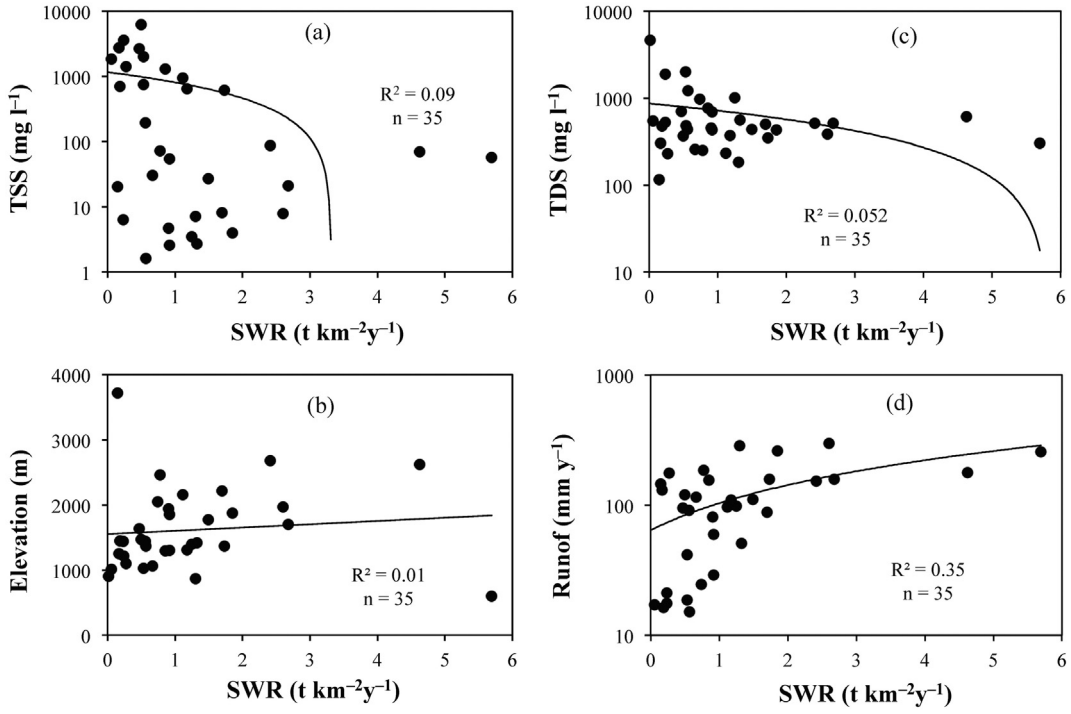

Fig. 8. Scatter plots of silicate weathering rates calculated for these inland rivers vs. various potential controlling variables. The linear regression analysis curves indicate weak correlations between SWR and some controlling factors.

Table 5
Comparison of chemical weathering rates in the Tibetan Plateau, Tianshan Mountains, and Qilian Mountains.

Areas	River basins	Locations	Geomorphology/environment	Mean annual precipitation (mm)	Mean annual evaporation (mm)	Runoff (mm y^{-1})	Mean annual temperature (°C)	Elevation (m)	SWR (t $km^{-2}y^{-1}$)	CWR (t $km^{-2}y^{-1}$)
Northern Tianshan	Yili R.	Middle reaches	High-mountains	200–350	1200–1400	287	5.0–8.1	867	1.30	7.39
	Yili R.	Middle reaches	Plain	350–500	1400–1600	257	7.5–8.4	599	5.69	6.05
Western Tianshan	Akesu R.	Lower reaches	Semi-desert	64	1890	177	9.2–11.5	1098	0.27	3.98
Southern Tianshan	Kuche R.	Lower reaches	Semi-desert	65–340	700–1350	120	10.7	1466	0.50	2.63
	Kaidu R.	Upper reaches	High-mountains	300–600	500–800	186	(−3.5)–(−6.5)	2464	0.78	6.52
		Lower reaches	Semi-desert	70–100	1100–1500	115	9.2–11.5	1065	0.67	3.96
Northern Tibetan Plateau	Yeerqiang R.	Upper and Middle	Alp and semi-desert	50–200	1300–2600	131–156	3.6–11.7	1249–3719	0.15–1.12	1.22–2.92
	Hetian R.	Middle reaches	Semi-desert	66.3–78.8	2030–2948	110–158	11.8–12.2	1313–1369	1.18–1.73	1.47–2.42
	Hetian R.	Lower reaches	Desert	5.4–89.6	2159–3137	17.4	11.3–11.5	1028	0.53	0.52
	Keliya R.	Middle reaches	Semi-desert	123	1840	98.1	9.5	1397	1.25	0.62
	Niya R.	Middle reaches	Semi-desert	51.0–53.4	2594–3916	95.2	10.7	1639	0.47	1.04
	Cheerchen R.	Middle reaches	Semi-desert	18.8–23.3	2046–2507	21.2	9.9–11.3	1214	0.24	0.97
Qilian Mt.	Heihe R.	Upper reaches	High-mountains	300–500	700	111–179	<2	1698–3782	1.49–4.62	5.74–11.7
		Lower reaches	Desert	50–100	2500–4000	2.77–29.2	8–10	907–1305	0.02–0.92	0.01–0.97
	Shiyang R.	Upper reaches	High-mountains	340–650	720–1200	88.5–298	0–5	1877–2215	1.70–2.60	5.36–13.4
		Lower reaches	Desert	100–150	2200–2640	16.3–41.7	>8	1444–1451	0.19–0.54	0.78–1.92
	Shule R.	Middle reaches	Semi-desert	50–200	1890	24.6–81.6	5.6	1938–2046	0.74–0.90	1.40–2.49
		Lower reaches	Desert	<50	2490–3033	15.1–17.6	6.9–8.8	1366–1437	0.23–0.57	0.66–0.83
Eastern/southeastern Tibetan Plateau	Yellow R.[a]	Upper reaches	High-mountains	430	1400	90.9–570	4	2323–4509	0.2–3.33	0.69–9.18
	Jinsha R.[b]	Upper reaches	High-mountains	200–500	517–642	25.8–83.6	(−6.7)–1.7	3530–4660	0.18–1.67	0.38–6.46
		Middle reaches	High-mountains	500–1000	591–871	243–322	(−4.6)–12.4	644–3035	1.72–2.84	6.73–8.52
		Lower reaches	Hills	1000–1200	1200–2034	346–347	16.5–20.9	306–644	3.31–3.7	6.88–13.3
	Mekong R.	Upper reaches[c]	High-mountains	279–668	543–649	230–430	(−4.4)–2.6	4330–4830	0.77–2.87	3.67–9.11
		Middle reaches[c]	High-mountains	328–1306	561–1042	251–952	(−3.6)–16.1	1456–3967	1.95–16.4	1.52–24.6
		Lower reaches[d]	Plain	1000–4000		423–591	26–30	5–1150	8.5–10.4	34.6–49.9
	Salween R.	Upper reaches[c]	High-mountains	310–431	528–604	56–369	(−5.4)–(−1.5)	4546–4925	0.77–4.58	0.51–11.0
		Middle reaches[c]	High-mountains	440–1108	609–1005	441–1343	(−1.7)–15.5	1850–4548	1.44–9.24	1.33–27.8
	Red R.[e]	Upper and Middle	High-mountains	800–1000	696–1200	43–108	15–18	1600–2200	3.5–10.6	
		Lower reaches	Plain	1500–2000		764–1025	>21	70–100	27.5	31.7
	Ganges	Upper reaches[f]	High-mountains	800–1600		1114–1554		2500–4900	13.5–18.9	50.4–144
		Estuary[g]	Plain	1500–2500		470		12	7.91	23.2
Southern Himalaya	Brahmaputra[h]	Middle reaches	High-mountains	200–400		168–181	2–14	2000–4729	0.5–2.5	3.99–14.1
		Syntaxis zone	High-mountains	4000–6000		3000–5000			34.2–38.0	
Western Himalaya	Indus[g]	Estuary	Plain	125–500		98			1.75	7.21

[a] Wu et al., 2005.
[b] Wu et al., 2008.
[c] Noh et al., 2009.
[d] Li et al., 2014b.
[e] Moon et al., 2007.
[f] Galy and France-Lanord, 1999.
[g] Gaillardet et al., 1999.
[h] Hren et al., 2007.

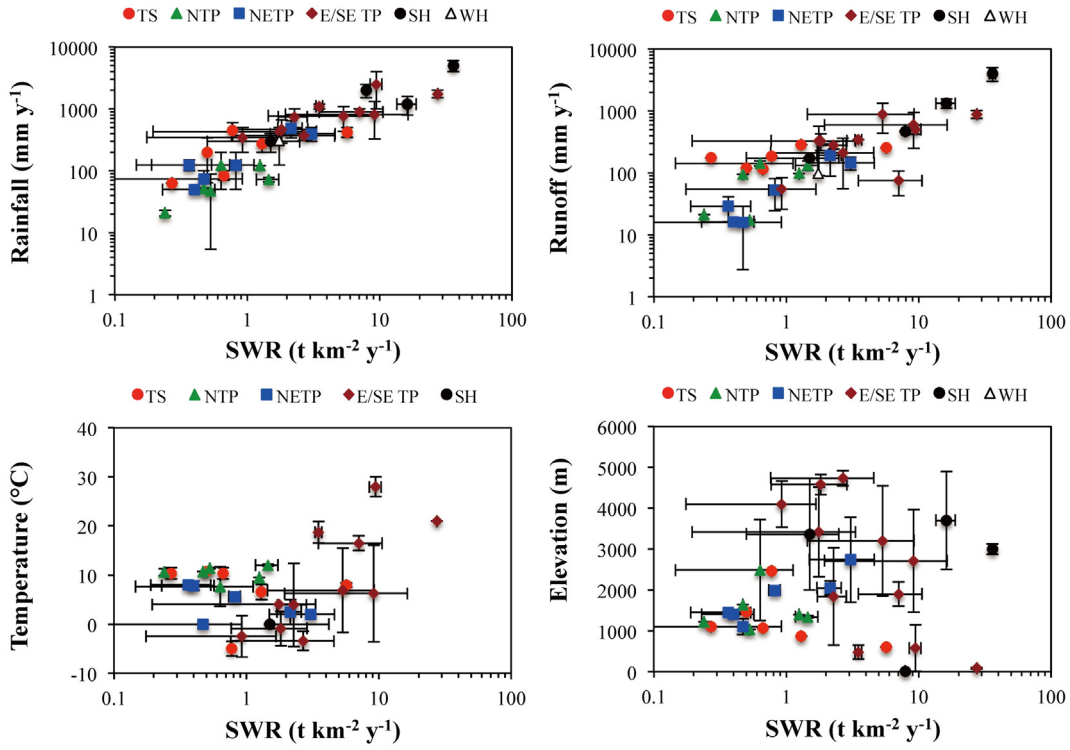

Fig. 9. Scatter plots of silicate chemical weathering rates (SWR) for Tibetan rivers vs. various potentially controlling variables. There seems to be good correlations between rainfall, runoff and SWR. TS: Tianshan, NTP: northern Tibetan Plateau, NETP: northeastern Tibetan Plateau, E/SE TP: eastern/southeastern Tibetan Plateau, SH: southern Himalaya, WH: western Himalaya.

References

Bickle, M.J., Bunbury, J., Chapman, H.J., Harris, N.B., Fairchild, I.J., Ahmad, T., 2003. Fluxes of Sr into the headwaters of the Ganges. Geochim. Cosmochim. Acta 67, 2567–2584.

Bickle, M.J., Chapman, H.J., Bunbury, J., Harris, N.B.W., Fairchild, I.J., Ahmad, T., Pomies, C., 2005. Relative contributions of silicate and carbonate rocks to riverine Sr fluxes in the headwaters of the Ganges. Geochim. Cosmochim. Acta 69, 2221–2240.

Bickle, M.J., Tipper, E.D., Galy, A., Chapman, H., Harris, N., 2015. On discrimination between carbonate and silicate inputs to Himalayan rivers. Am. J. Sci. 315, 120–166.

Blum, J.D., Gazis, C.A., Jacobson, A.D., Chamberlain, C.P., 1998. Carbonate versus silicate weathering in the Raikhot watershed within the high Himalayan crystalline series. Geology 26, 411–414.

Chapman, H., Bickle, M., Thaw, S.H., Thiam, H.N., 2015. Chemical fluxes from time series sampling of the Irrawaddy and Salween rivers, Myanmar. Chem. Geol. 401, 15–27.

Chen, J.S., Wang, F.Y., Xia, X.H., Zhang, L.T., 2002. Major element chemistry of the Changjiang (Yangtze River). Chem. Geol. 187, 231–255.

Chetelat, B., Liu, C.Q., Zhao, Z.Q., Wang, Q.L., Li, S.L., Li, J., Wang, B.L., 2008. Geochemistry of the dissolved load of the Changjiang Basin rivers: anthropogenic impacts and chemical weathering. Geochim. Cosmochim. Acta 72, 4254–4277.

China Geological Survey, 2004. Geological map of the People's Republic of China 1:2 500 000. SinoMaps Press, Beijing.

Feng, Q., Liu, W., Su, Y.H., Zhang, Y.W., Si, J.H., 2004. Distribution and evolution of water chemistry in Heihe River basin. Environ. Geol. 45, 947–956.

Gaillardet, J., Dupre, B., Louvat, P., Allegre, C.J., 1999. Global silicate weathering and CO_2 consumption rates deduced from the chemistry of large rivers. Chem. Geol. 159, 3–30.

Galy, A., France-Lanord, C., 1999. Weathering processes in the Ganges–Brahmaputra basin and the riverine alkalinity budget. Chem. Geol. 159, 31–60.

Galy, A., France-Lanord, C., 2001. Higher erosion rates in the Himalaya: geochemical constraints on riverine fluxes. Geology 29, 23–26.

Gao, Q.Z., Tao, Z., Huang, X.K., Nan, L., Yu, K.F., Wang, Z.G., 2009. Chemical weathering and CO_2 consumption in the Xijiang River basin, South China. Geomorphology 106, 324–332.

Harris, N., Bickle, M., Chapman, H., Fairchild, I., Bunbury, J., 1998. The significance of Himalayan rivers for silicate weathering rates: evidence from the Bhote Kosi tributary. Chem. Geol. 144, 205–220.

Hren, M.T., Chamberlain, C.P., Hilley, G.E., Blisniuk, P.M., Bookhagen, B., 2007. Major ion chemistry of the Yarlung Tsangpo–Brahmaputra river: chemical weathering, erosion, and CO_2 consumption in the southern Tibetan Plateau and eastern syntaxis of the Himalaya. Geochim. Cosmochim. Acta 71, 2907–2935.

Hydrology and Water Resources Bureau of Gansu Province, 2012. Water Resources Bulletin in Gansu Province (in Chinese).

Jiang, L., Yao, Z., Wang, R., Liu, Z., Wang, L., Wu, S., 2015. Hydrochemistry of the middle and upper reaches of the Yarlung Tsangpo River system: weathering processes and CO_2 consumption. Environ. Earth Sci. http://dx.doi.org/10.1007/s12665-015-4237-6.

Kadeer, 1982. Multi-year variations analysis of water discharge in the Yili River. Xinjiang Geol. Z1, 46–50 (in Chinese).

Karim, A., Veizer, J., 2000. Weathering processes in the Indus River basin: implications from riverine carbon, sulfur, oxygen, and strontium isotopes. Chem. Geol. 170, 153–177.

Li, S.L., Chetelat, B., Yue, F.J., Zhao, Z.Q., Liu, C.Q., 2014a. Chemical weathering processes in the Yalong River draining the eastern Tibetan Plateau, China. J. Asian Earth Sci. 88, 74–84.

Li, S.Y., Lu, X.X., Bush, R.T., 2014b. Chemical weathering and CO_2 consumption in the lower Mekong River. Sci. Total Environ. 472, 162–177.

Li, X.Q., Gan, Y.Q., Zhou, A.G., Liu, Y.D., Wang, D., 2013. Hydrological controls on the sources of dissolved sulfate in the Heihe River, a large inland river in the arid northwestern China, inferred from S and O isotopes. Appl. Geochem. 35, 99–109.

Ma, J., Zhang, P., Zhu, G., Wang, Y., Edmunds, W.M., Ding, Z., He, J., 2012. The composition and distribution of chemicals and isotopes in precipitation in the Shiyang River system, northwestern China. J. Hydrol. 436-437, 92–101.

Manaka, T., Otani, S., Inamura, A., Suzuki, A., Aung, T., Roachanakanan, R., Ishiwa, T., Kawahata, H., 2015. Chemical Weathering and Long-Term CO_2 Consumption in the Ayeyarwady and Mekong River Basins in the Himalayas. Biogeosciences, n/a-n/a, Journal of Geophysical Research.

Meybeck, M., 1987. Global chemical weathering of surficial rocks estimated from river dissolved loads. Am. J. Sci. 287, 401–428.

Meybeck, M., 1993. Riverine transport of atmospheric carbon — sources, global typology and budget. Water Air Soil Pollut. 70, 443–463.

Meybeck, M., Helmer, R., 1989. The quality of rivers — from pristine stage to global pollution. Glob. Planet. Chang. 75, 283–309.

Millot, R., Gaillardet, J.É., Dupré, B., Allègre, C.J., 2003. Northern latitude chemical weathering rates: clues from the Mackenzie River basin, Canada. Geochim. Cosmochim. Acta 67, 1305–1329.

Moon, S., Huh, Y., Qin, J.H., van Pho, N., 2007. Chemical weathering in the Hong (red) River basin: rates of silicate weathering and their controlling factors. Geochim. Cosmochim. Acta 71, 1411–1430.

National Administration of Surveying, Mapping and Geoinformation (NASG), 2006o. The Maps of China—River Systems. SinoMaps Press, Beijing.

Negrel, P., Allegre, C.J., Dupre, B., Lewin, E., 1993. Erosion sources determined by inversion of major and trace-element ratios and strontium isotopic-ratios in river water — the Congo basin case. Earth Planet. Sci. Lett. 120, 59–76.

Noh, H., Huh, Y., Qin, J.H., Ellis, A., 2009. Chemical weathering in the three rivers region of eastern Tibet. Geochim. Cosmochim. Acta 73, 1857–1877.

Oliva, P., Viers, J., Dupre, B., 2003. Chemical weathering in granitic environments. Chem. Geol. 202, 225–256.

Qin, J., Huh, Y., Edmond, J., Du, G., Ran, J., 2006. Chemical and physical weathering in the Min Jiang, a headwater tributary of the Yangtze River. Chem. Geol. 227, 53–69.

Raymo, M.E., Ruddiman, W.F., 1992. Tectonic forcing of late Cenozoic climate. Nature 359, 117–122.

Raymo, M.E., Ruddiman, W.F., Froelich, P.N., 1988. Influence of late Cenozoic mountain building on ocean geochemical cycles. Geology 16, 649–653.
Roy, S., Gaillardet, J., Allègre, C.J., 1999. Geochemistry of dissolved and suspended loads of the Seine River, France: anthropogenic impact, carbonate and silicate weathering. Geochim. Cosmochim. Acta 63, 1277–1292.
Ruddiman, W.F., Kutzbach, J.E., 1989. Forcing of late Cenozoic northern hemisphere climate by plateau uplift in southern Asia and the American west. J. Geophys. Res.-Atmos. 94, 18409–18427.
Ruddiman, W.F., Prell, W.L., 1997. Introduction to the Uplift-Climate Connection. pp. 3–15.
Singh, S.K., Sarin, M.M., France-Lanord, C., 2005. Chemical erosion in the eastern Himalaya: major ion composition of the Brahmaputra and delta C-13 of dissolved inorganic carbon. Geochim. Cosmochim. Acta 69, 3573–3588.
Sun, J.Y., Qin, D.H., Ren, J.W., Li, Z.Q., Hou, S.G., 2002. A study of water chemistry and aerosol at the headwaters of the Urumqi River in the Tianshan mountains. J. Glaciol. Geocryol. 24, 186–191.
Wang, B., Lee, X.Q., Yuan, H.L., Zhou, H., Cheng, H.G., Cheng, J.Z., Zhou, Z.H., Xing, Y., Fang, B., Zhang, L.K., Yang, F., 2012. Distinct patterns of chemical weathering in the drainage basins of the Huanghe and Xijiang River, China: evidence from chemical and Sr-isotopic compositions. J. Asian Earth Sci. 59, 219–230.
Wang, W.X., Xu, P.J., 2009. Research progress in precipitation chemistry in China. Prog. Chem. 21, 266–281.
White, A.F., Blum, A.E., 1995. Effects of climate on chemical-weathering in watersheds. Geochim. Cosmochim. Acta 59, 1729–1747.
Wu, L.L., Huh, Y., Qin, J.H., Du, G., van der Lee, S., 2005. Chemical weathering in the Upper Huang He (Yellow River) draining the eastern Qinghai–Tibet Plateau. Geochim. Cosmochim. Acta 69, 5279–5294.
Wu, W.H., Xu, S.J., Yang, J.D., Yin, H.W., 2008a. Silicate weathering and CO_2 consumption deduced from the seven Chinese rivers originating in the Qinghai–Tibet Plateau. Chem. Geol. 249, 307–320.
Wu, W.H., Yang, J.D., Xu, S.J., Yin, H.W., 2008b. Geochemistry of the headwaters of the Yangtze rRiver, Tongtian He and Jinsha iang: silicate weathering and CO_2 consumption. Appl. Geochem. 23, 3712–3727.
Wu, W.H., Zheng, H.B., Yang, J.D., Luo, C., Zhou, B., 2013. Chemical weathering, atmospheric CO_2 consumption, and the controlling factors in a subtropical metamorphic-hosted watershed. Chem. Geol. 356, 141–150.
Xiao, J., Jin, Z.D., Ding, H., Wang, J., Zhang, F., 2012. Geochemistry and solute sources of surface waters of the Tarim River basin in the extreme arid region, NW Tibetan Plateau. J. Asian Earth Sci. 54-55, 162–173.
Xijiang Tarim River Basin Management Bureau, 2003. Water Resources Bulletin of Tarim River (in Chinese).
Xu, M., Lu, A.H., Xu, F., Wang, B., 2008. Seasonal chemical composition variations of wet deposition in Urumchi, northwestern China. Atmos. Environ. 42, 1042–1048.
Xu, Z.F., Liu, C.Q., 2007. Chemical weathering in the upper reaches of Xijiang River draining the Yunnan–Guizhou Plateau, southwest China. Chem. Geol. 239, 83–95.
Yang, Q., Xiao, H.L., Zhao, L.J., Yang, Y.G., Li, C.Z., Zhao, L.A., Yin, L., 2011. Hydrological and isotopic characterization of river water, groundwater, and groundwater recharge in the Heihe River basin, northwestern China. Hydrol. Process. 25, 1271–1283.
Zhang, J., Takahashi, K., Wushiki, H., Yabuki, S., Xiong, J.M., 1995. Water geochemistry of the rivers around the Taklimakan Desert (Nw China) — crustal weathering and evaporation processes in arid-land. Chem. Geol. 119, 225–237.
Zhang, Q., Jin, Z., Zhang, F., Xiao, J., 2015. Seasonal variation in river water chemistry of the middle reaches of the Yellow River and its controlling factors. J. Geochem. Explor. 156, 101–113.
Zhao, Z.P., Tian, L., Fischer, E., Li, Z.Q., Jiao, K.Q., 2008. Study of chemical composition of precipitation at an alpine site and a rural site in the Urumqi River Valley, Eastern Tien Shan, China. Atmos. Environ. 42, 8934–8942.
Zhu, B.Q., Yang, X.P., 2007. The ion chemistry of surface and ground waters in the Taklimakan Desert of Tarim Basin, western China. Chin. Sci. Bull. 52, 2123–2129.
Zhu, B.Q., Yang, X.P., Rioual, P., Qin, X.G., Liu, Z.T., Xiong, H.G., Yu, J.J., 2011. Hydrogeochemistry of three watersheds (the Erlqis, Zhungarer and Yili) in northern Xinjiang, NW China. Appl. Geochem. 26, 1535–1548.
Zhu, B.Q., Yu, J.J., Qin, X.G., Rioual, P., Xiong, H.G., 2012. Climatic and geological factors contributing to the natural water chemistry in an arid environment from watersheds in northern Xinjiang, China. Geomorphology 153, 102–114.
Zhu, G.F., Su, Y.H., Feng, Q., 2008. The hydrochemical characteristics and evolution of groundwater and surface water in the Heihe River basin, northwest China. Hydrogeol. J. 16, 167–182.